$$r_{FT}=\frac{k_c P_{CO} P_{H_2}}{(1+cP_{CO})^2} \qquad (69)$$

2.5 Vapor-Liquid Equilibrium Calculations in Fischer-Tropsch Synthesis:

The major constituents of the products from Fischer-Tropsch synthesis are the hydrocarbons ranging from methane to high melting paraffins with relatively small quantities of olefinic compounds. For iron catalyst, carbon dioxide is one of the major products formed with relatively small amounts of product water. In the case of cobalt catalyst, however, due to its poor activity for water gas shift reaction, water will be the major byproduct with relatively small amount of carbon dioxide. Small quantities of other byproducts such as alcohols, aldehydes, ketones etc. are also formed. Straight-chain paraffins along with some 2-methylated branched paraffins predominate among the saturated hydrocarbons; major olefins are terminal olefins.

The products and the unreacted synthesis gas leaving the top of the slurry reactor will be assumed to be in equilibrium with the liquid phase in the reactor. A computer program has been developed to study the phase equilibria of the vapor and the liquid streams leaving the slurry reactor. Such information will be helpful in determining the relative flow rates and the composition of vapor and liquid streams which can be further used in the process design of the downstream units in the Fischer-Tropsch Plant. The conversion and the production yields from the slurry reactor model will be used to determine the overall composition for the phase

equilibrium calculations. The problem presented here is identical with that of determining vapor and liquid compositions in a multi-component flash separation. Following assumptions will be made regarding the products formed during the reaction. The hydrocarbon products consists of n-alkanes and n-alkenes only. These are, in fact, the main products for many of the FT catalyst and little design error will be introduced by lumping the methyl-branched isomers with n-alkanes and n-alkenes. In the lower oxygenates, ketones and primary alcohols are formed in relatively small amounts as compared to water and hence these compounds will be lumped with water. The light hydrocarbons (C_5 to C_{11}) will be lumped together; heavy hydrocarbons (C_{12} to C_{15}) will be lumped together and hydrocarbons C_{16} and heavier will be considered as the slurry reactor wax with an average composition of C_{40} paraffin. The olefin to paraffin split of the hydrocarbon products can be obtained from the literature. For example, unreacted synthesis gas and reaction products from the Mobil's pilot plant for Fischer-Tropsch synthesis may be characterized into following fourteen components:

Component No.	Component(s)
1	Carbon Dioxide
2	Water + Ketones & Primary Alcohols (Acetone & 1-Propanol)
3	Hydrogen
4	Carbon Monoxide
5	Methane
6	Ethylene
7	Ethane

8	Propylene
9	n-Propane
10	Butylene
11	n-Butane
12	C_5 to C_{11} Light Hydrocarbons Lumped as n-Octane
13	C_{12} to C_{15} Heavy Hydrocarbons as n-Tridecane
14	C_{16} and Heavier as Slurry Reactor Wax (C_{40} Paraffin)

Phase Equilibrium Calculations for Multicomponent Vapor-Liquid Phase Equilibria:

A technique has been presented by Bendale, 1991, to predict multicomponent vapor-liquid equilibria from the optimized binary interaction parameters obtained from the Peng-Robinson equation of state, which is given as:

$$P = \frac{RT}{(V - b_{mix})} - \frac{a_{mix}}{V(V + b_{mix}) + b_{mix}(V - b_{mix})} \tag{70}$$

For a multicomponent mixture, the parameters a_{mix} and b_{mix} are given by the following expressions:

$$a_{mix} = \sum_i \sum_j x_i x_j \sqrt{a_i a_j}\,(1 - \delta_{ij}) \tag{71}$$

$$b_{mix} = \sum_i x_i b_i \tag{72}$$

In the above equation, δ_{ij} is defined as an interaction parameter that describes the deviation of parameter a_{mix} from the geometric mean of the pure component parameters a_i and a_j and is assumed to be constant. The pure component parameters a_i and b_i are given as:

$$a_i = a(T_c)\,\alpha(T_r, \omega) \tag{73}$$

$$a(T_c) = 0.45724\,(R^2 T_c^2 / P_c) \tag{74}$$

$$\alpha(T_r, \omega) = [1 + \kappa\,(1 - \sqrt{T_r})]^2 \tag{75}$$

$$\kappa = C_a\,(0.37464 + 1.54226\,\omega - 0.26992\,\omega^2) \tag{76}$$

If ω is greater than 0.5, then

$$\kappa = C_a\,(0.379642 + 1.48503\,\omega - 0.164423\,\omega^2 + 0.016666\,\omega^3) \tag{77}$$

$$b_i = C_b\,[0.0778\,(RT_c / P_c)] \tag{78}$$

The optimized values of correction factors C_a and C_b for pure components are evaluated which minimize the sum of absolute relative errors of calculated and experimental saturated vapor pressure and saturated liquid density. The values of these correction factors approach unity for small molecules and non-polar gases which the Peng-Robinson equation of state is known to model accurately. If these values are not available, then the default values are assigned as unity.

The expression for the fugacity coefficient obtained from the evaluation of the following equation,

$$RT\ln\Phi_i = \int_V^{\infty}[(\frac{\partial P}{\partial n_i}) - \frac{RT}{V}]\,dV - RT\ln Z \tag{79}$$

is given as:

$$\ln\Phi_i = \frac{b_i}{b_{mix}}(Z-1) - \ln(Z-B)$$

$$+ [\frac{\sum_k x_k(a_{ik}+a_{ki})}{a_{mix}} - \frac{b_i}{b_{mix}}] \times \frac{a_{mix}}{2.414bRT}\ln[\frac{Z-0.414B}{Z+2.414B}] \tag{80}$$

$$B = \frac{b_{mix}P}{RT} \tag{81}$$

Phase equilibrium calculations are performed at constant temperature and pressure and known overall composition to determine the flow rates and compositions of vapor and liquid streams. The governing equations include overall and component material balances, mole fraction constraints, and thermodynamic equilibrium criterion of equal fugacities of each component in each phase. For an N component system at constant temperature and pressure, there will be 2N independent expressions for these components equilibrated in two phases, with 2N unknowns, L, V, x_i's and y_i's, respectively.

On the basis of one mole of mixture F (unreacted reactants and products formed), an overall material balance and a component balance for each component can be represented as follows:

$$L + V = F = 1 \tag{82}$$

$$L x_i + V y_i = F z_i = z_i, \qquad i = 1 \, to \, N \tag{83}$$

with the following constraints:

$$\sum_i z_i = \sum_i x_i = \sum_i y_i = 1, \qquad i = 1 \, to \, N \tag{84}$$

and thermodynamic criteria,

$$f_i^V = f_i^L \quad or \quad \phi_i^V y_i P = \phi_i^L x_i P \quad or \quad \phi_i^V y_i = \phi_i^L x_i, \quad i = 1 \, to \, N \tag{85}$$

To perform Flash calculations, temperature T and pressure P are considered as the known variables, which are used to calculate the unknown mole fractions x_i's and y_i's of the liquid and vapor phases, respectively. In addition to system temperature and pressure, the input data required consists of critical temperature, critical pressure and acentric factor of each component as well as the optimized binary interaction parameters, δ_{ij} as applied to the Peng-Robinson equation of state. The liquid and vapor phase fugacity coefficients for each component can be readily calculated from the expression 80. The set of equations 82, 83, 84 and 85 are solved simultaneously to determine the flow rates and mole fractions of liquid and vapor streams.

3.0 Development of Computer Codes:

The model equations for the Fischer-Tropsch synthesis reactor constitute a set of coupled second-order non-linear differential equations. These equations are not amenable to an analytical solution and therefore, a numerical method was selected for solution. Orthogonal collocation techniques are particularly suitable for the solution of boundary value problems and the software package, COLSYS, developed by Ascher et al. (1981) was selected for the numerical solution of the model equations. This method is based on spline collocation at Gaussian points using a B-spline basis. Approximate solutions are computed on a sequence of automatically selected meshes until a user-specified set of tolerances is satisfied.

Computer codes for the reactor model have been developed with a modular approach to computer programming, to ensure easy modifications by the user. Standard FORTRAN 77 has been used for writing the codes since this will ensure transfer to other compatible systems. The codes have been tested on VAX/VMS operating system and personal computers. Appendix-A gives the system requirements and operating instructions for personal computers. Computer codes for the slurry reactor model have been developed for the following cases:

With external recirculation of slurry

- Gas plug flow; Liquid axial dispersion
- Gas axial dispersion; Liquid axial dispersion

No external recirculation of slurry

- o Gas plug flow; Liquid axial dispersion
- o Gas axial dispersion; Liquid axial dispersion

3.1 Test and Validation of Reactor Models:

Both methanol synthesis and Fischer-Tropsch synthesis models were tested against available experimental data from demonstration and process development units.

Methanol Synthesis

For methanol synthesis, Air products and Chemicals conducted process development unit runs in a slurry reactor to investigate the influence of different operating conditions on methanol production rates. The range of operating variables investigated are summarized in Table 3.

Table 3. Operating conditions and reactor dimensions for process development unit for methanol synthesis

Diameter	0.57 m
Length	5.85 m
Temperature	235-285°C
Pressure	35-62 atm
Gas Velocity	0.04-0.194 m/sec

Table 3. Cont'd

Slurry Conc.	28.0-42.0 wt. %
H_2/CO ratio	0.5-2.6
CO_2 Conc.	0.9-12 %

Air Products PDU reactor for methanol synthesis was simulated using our reactor model. The kinetic expressions of Berty et al. (1983), Wedel et al. (1988) and Graff et al. (1988) were tested in the model. None of these kinetic expressions could predict the high production rates achieved for PDU runs. The predicted rates were lowest for Berty et al. (1983) model followed by Graff et al. (1988) and Wedel et al. (1988) models. These kinetic expressions were again tested in the reactor model by adjusting the rate constants to match the experimental production rate for a run where mass transfer effects were expected to be negligible (i.e. high gas velocity and low slurry concentration). The kinetic expressions of Berty et al. (1983) and Graff et al. (1988) could not predict the effects of temperature, hydrogen concentration and carbon dioxide concentrations. The Wedel et al. (1988) power law expression could well predict the effect of temperature and hydrogen concentration. The influence of carbon dioxide concentration was not accounted for, since the reported expression is based on data obtained with more than optimum carbon dioxide concentration. Suitable correction factors for the effect of lower carbon dioxide concentrations were, therefore incorporated into the model based on literature information. It was observed that for slurry concentration lower than 35 wt. % and gas velocities higher than 0.1 m/s, the predicted rates were generally within 6% of the experimental rates. Figure 1 is a parity plot of production rates for 22 such runs. The predicted rates were, however, high for gas velocities below 0.05

m/s for all slurry concentrations. The predicted rates were always higher for slurry concentrations higher than 35 wt%. As shown in Figure 2, for a given gas velocity, the relative error increased with increasing slurry concentration. Also for a given slurry concentration relative error decreased with increasing gas velocity. The low production rates observed at high slurry concentrations and low gas velocities could be the result of reduced gas-liquid mass transfer rate due to poor gas-liquid contact in some parts of the reactor (mainly distributor region). The available literature correlations could not, however, predict the large decreases in volumetric mass transfer coefficient required to predict the experimental reactor performances. Further work is needed to investigate the changes in mixing patterns and gas-liquid contacting with increasing slurry concentrations in large diameter columns.

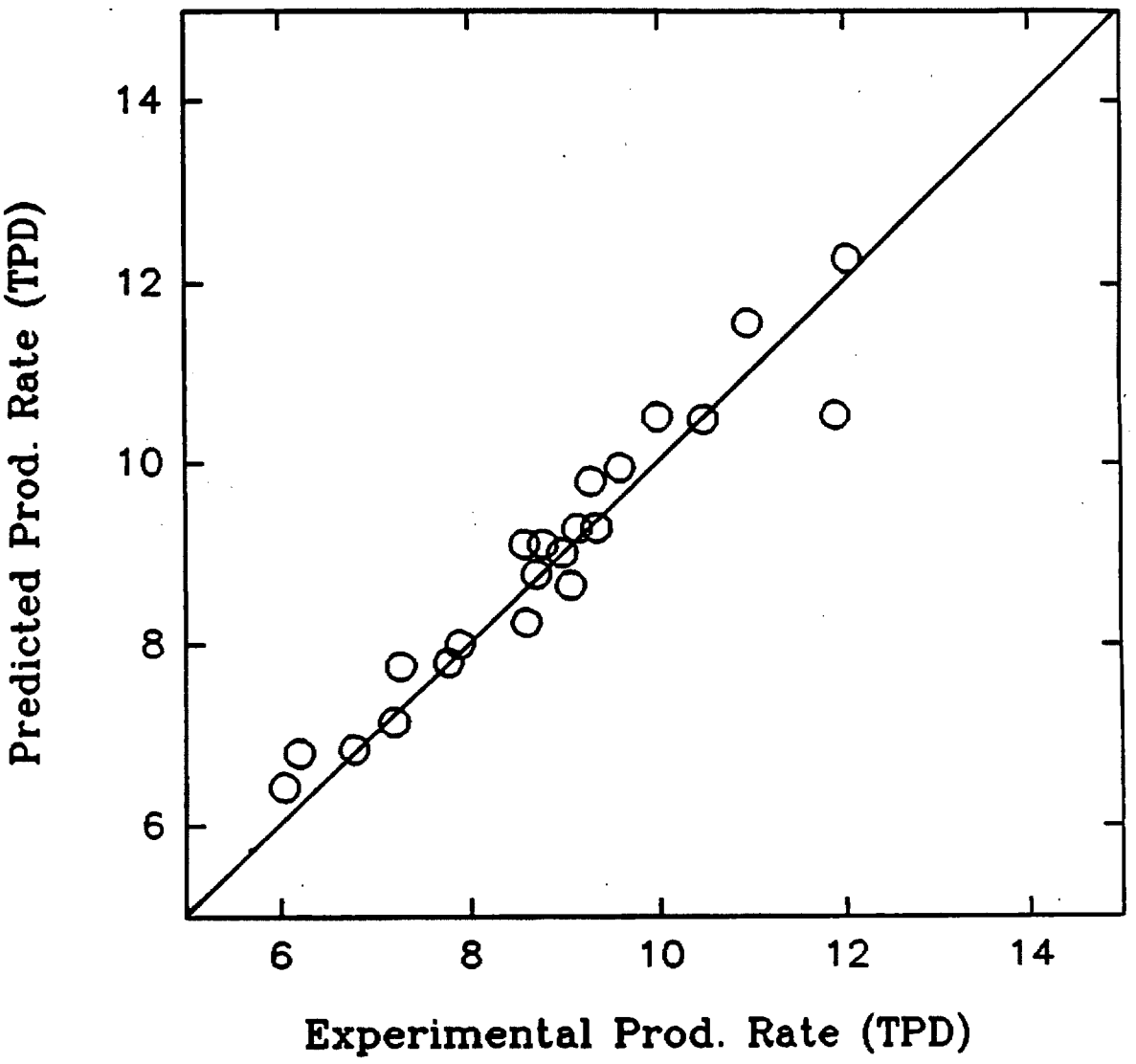

Figure 1. Predicted vs experimental production rates for PDU

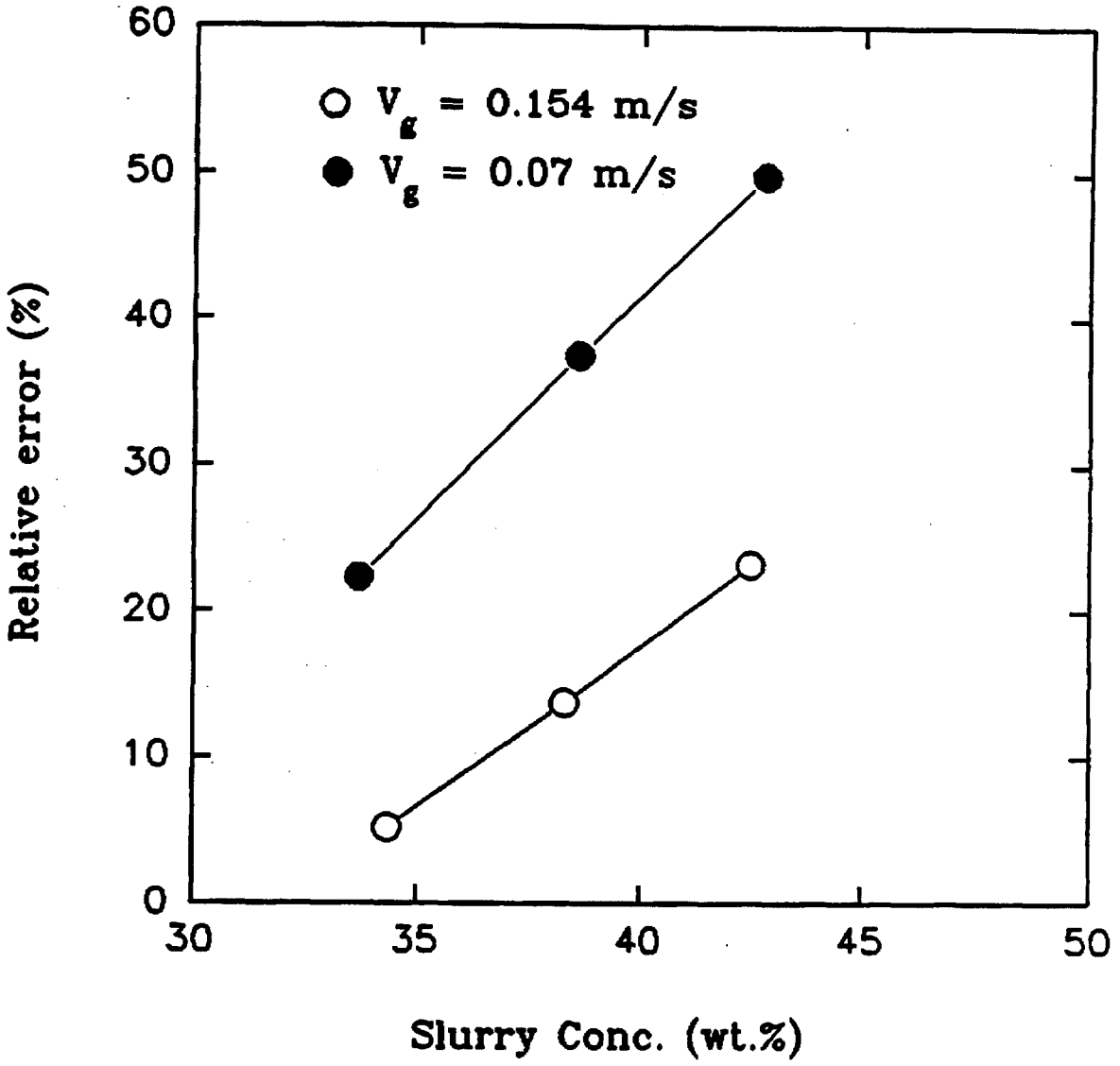

Figure 2. Effects of slurry concentration on relative error between predicted and experimental rates

Effect of Operating Variables

The reactor model for methanol synthesis was also used to investigate the effect of operating variables. For the results of this section, the slurry reactor was modeled assuming there was no external recirculation of slurry and both gas and liquid phases were axially dispersed. Table 4 gives the range of operating variables studied.

Table 4. Range of input data used to simulate slurry Fischer-Tropsch reactor

Diameter	4.8 m
Length	14.5 m
Temperature	232-265 °C
Pressure	50-70 atm
Gas Velocity	0.10-0.16 m/s
Slurry Conc.	30-35 wt.%
Syngas in Feed	90.0%
H_2/CO ratio	0.5-2.0
Particle size	0.000025-0.00005 m

Figure 3 shows that methanol production rate increases with increasing reactor temperature, up to a temperature of about 240°C. Production rate, however, decreased sharply at higher temperatures due to increasing rate of backward reaction. Figure 4 shows that methanol production rate increased linearly with reactor pressure while syngas conversion increased only

slightly with increasing reactor pressure. Figure 5 shows that while the production rate increased linearly with space velocity, the syngas conversion decreased with increasing space velocity. Methanol production rate increased linearly with increasing hydrogen to carbon monoxide ratio upto a ratio of about one (Figure 6). The rate of increase dropped for higher hydrogen to carbon monoxide ratios.

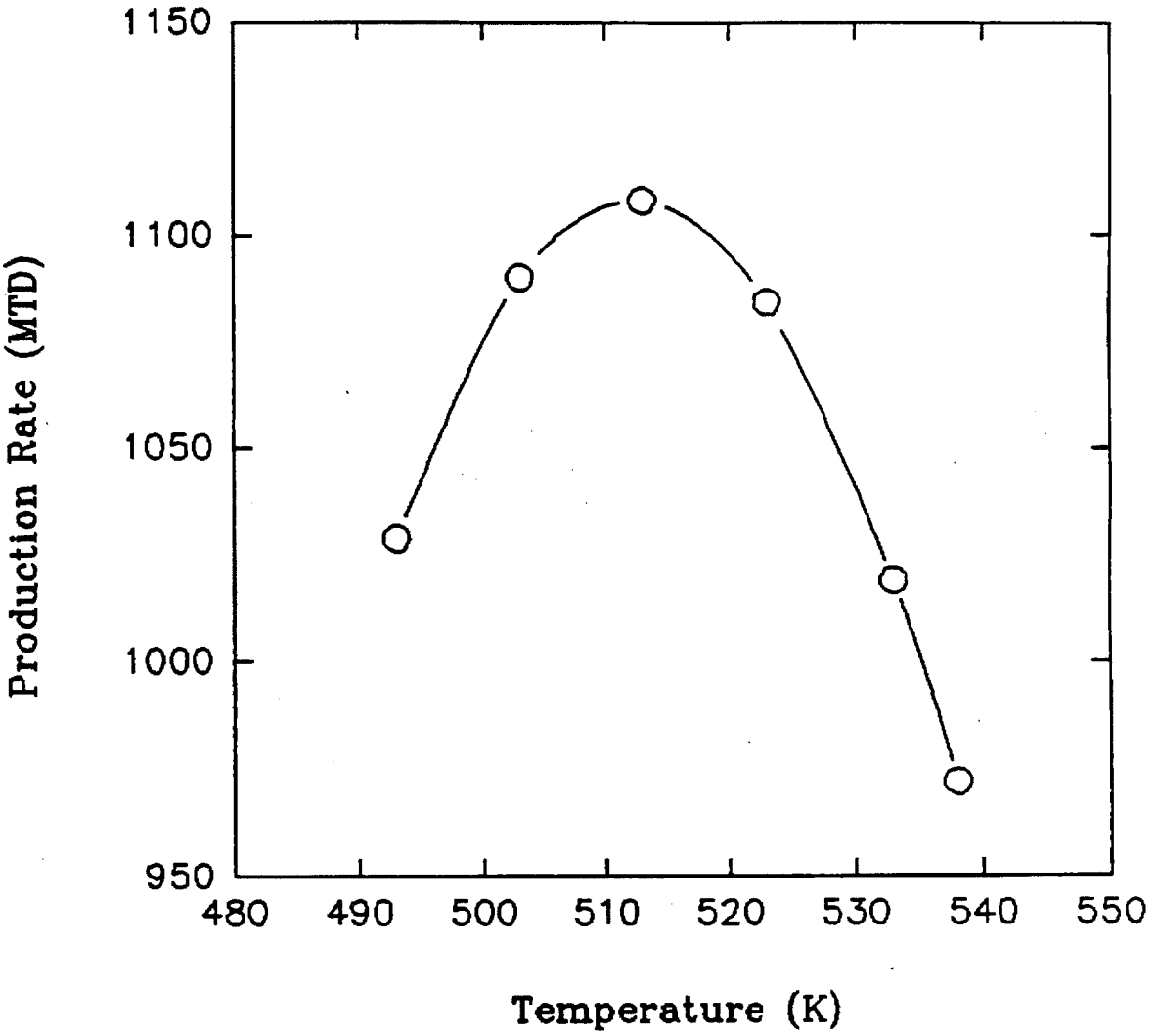

Figure 3. Effect of temperature on methanol production rate

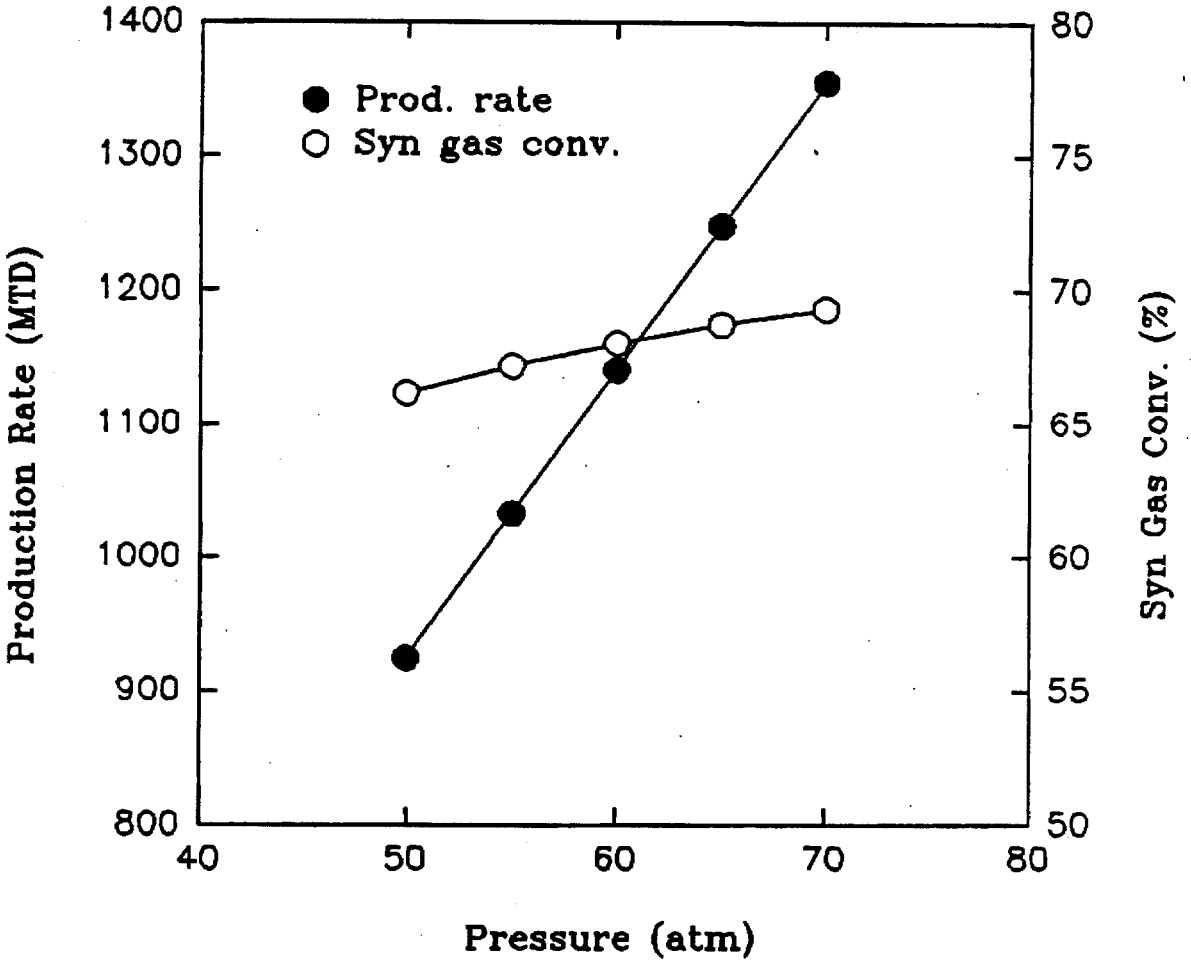

Figure 4. Effect of pressure on methanol production rate and hydrogen conversion

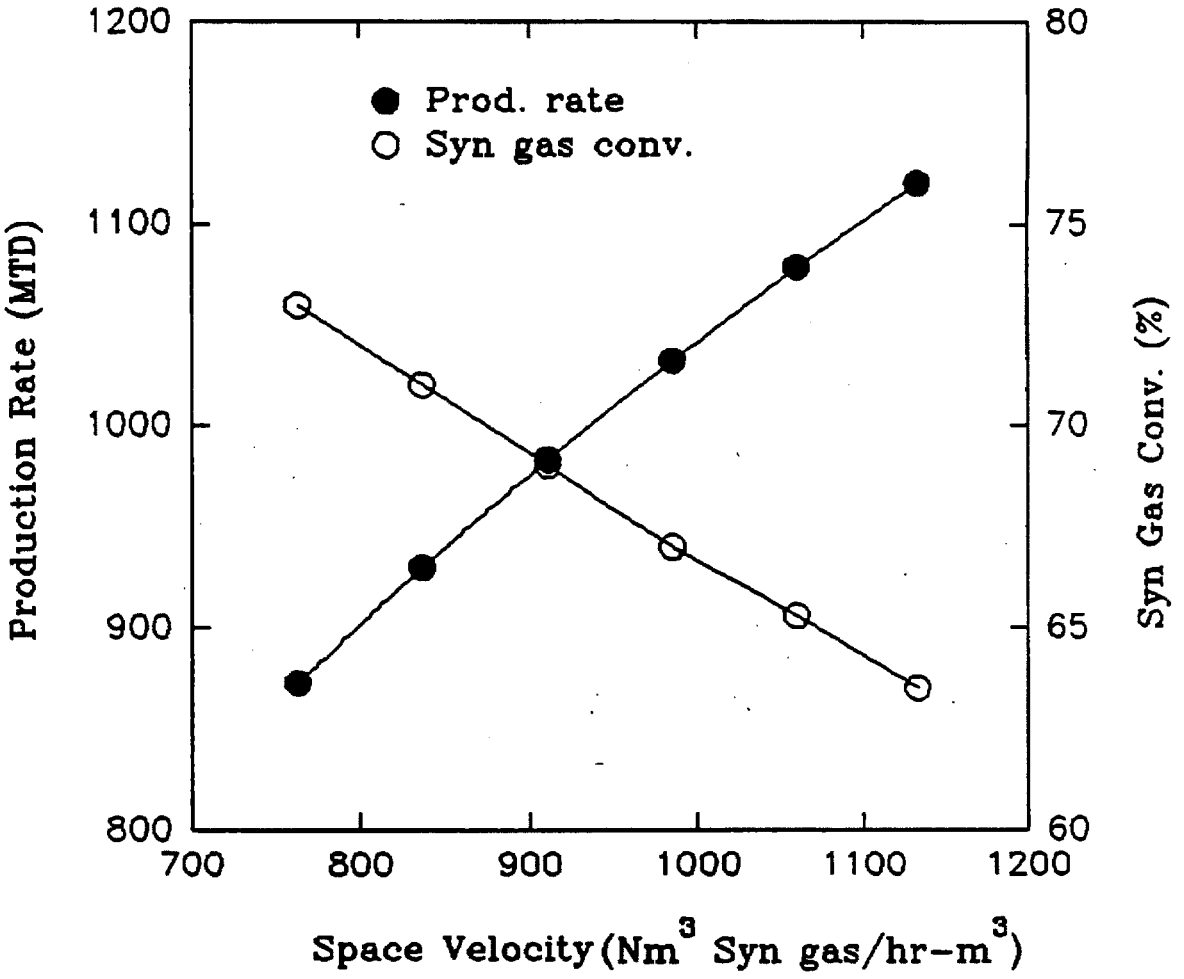

Figure 5. Effect of space velocity on methanol production rate and syn gas conversion.

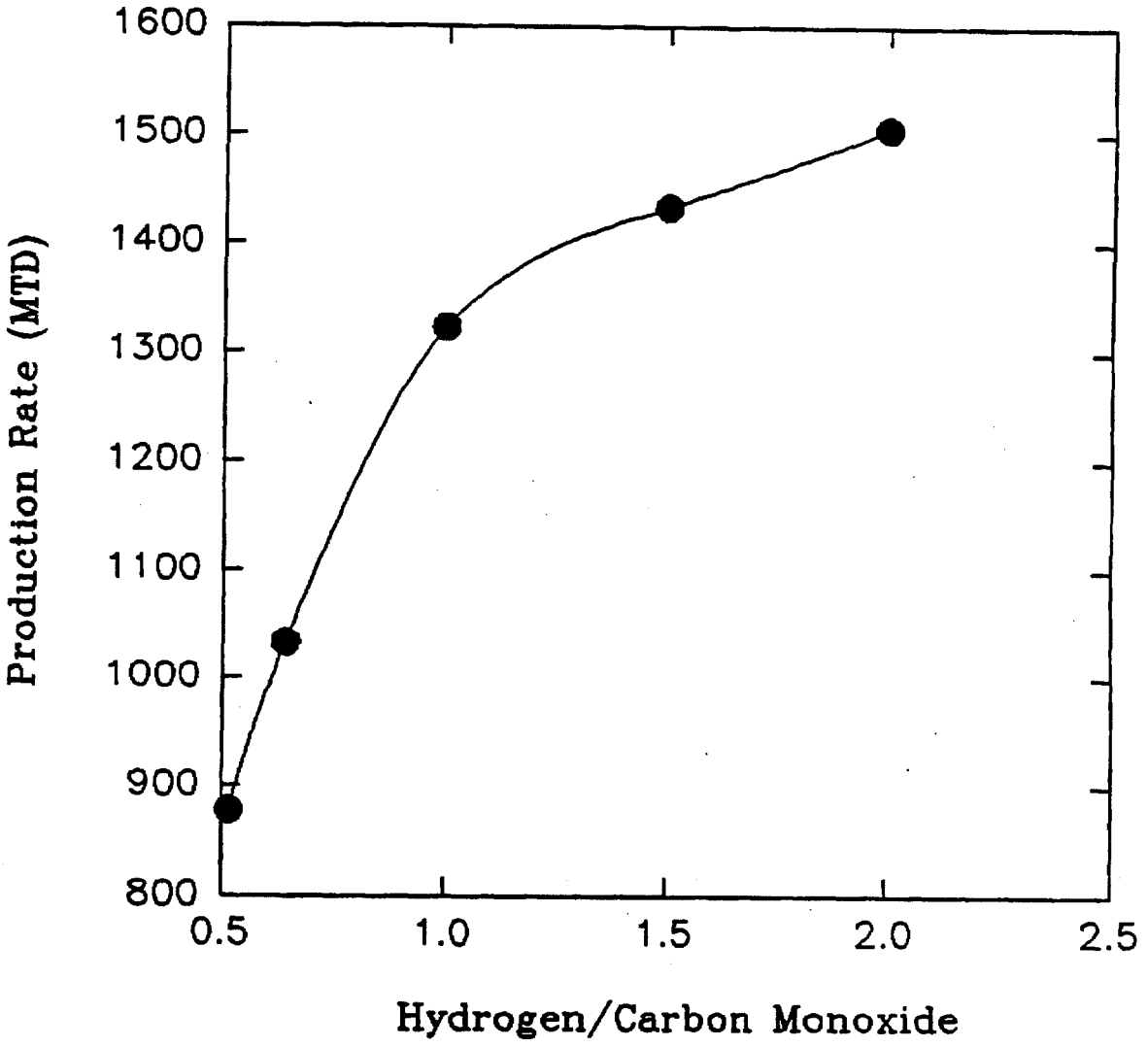

Figure 6. Effect of hydrogen to carbon monoxide ratio on methanol production rate.

Parameter Sensitive Analysis

Computer simulation models allow the user to perform parameter sensitivity analysis and calculate estimated errors. For example it is possible to quantify error in predicted reactor productivity due to an estimated error in gas holdup. Parameter sensitive analysis was carried out to investigate the effects of non-adjustable variables such as gas holdup, volumetric mass transfer coefficient and gas phase dispersion coefficient.

Figure 7 shows that both production rate and syngas conversion decreased with increasing gas holdup. It can also be observed that a 14% error in gas holdup estimate could result in about 3% error in estimated production rate for a commercial size reactor. Figure 8 shows that production rate increases with increasing mass transfer coefficient, the rate of increase, however, slows down when volumetric mass transfer coefficient increases above 0.45 s^{-1}. In this region the overall rate is no longer limited by mass transfer. The volumetric mass transfer coefficient estimated by the selected correlation in the model is also shown on Figure 8. The reactor production rate decreased with increasing gas phase dispersion coefficient (Figure 9). As the dispersion coefficient increases the reactor approaches the behavior of a single CSTR. For a commercial size slurry reactor, a 100% error in estimated dispersion coefficient would result in about 2% error in production rate.

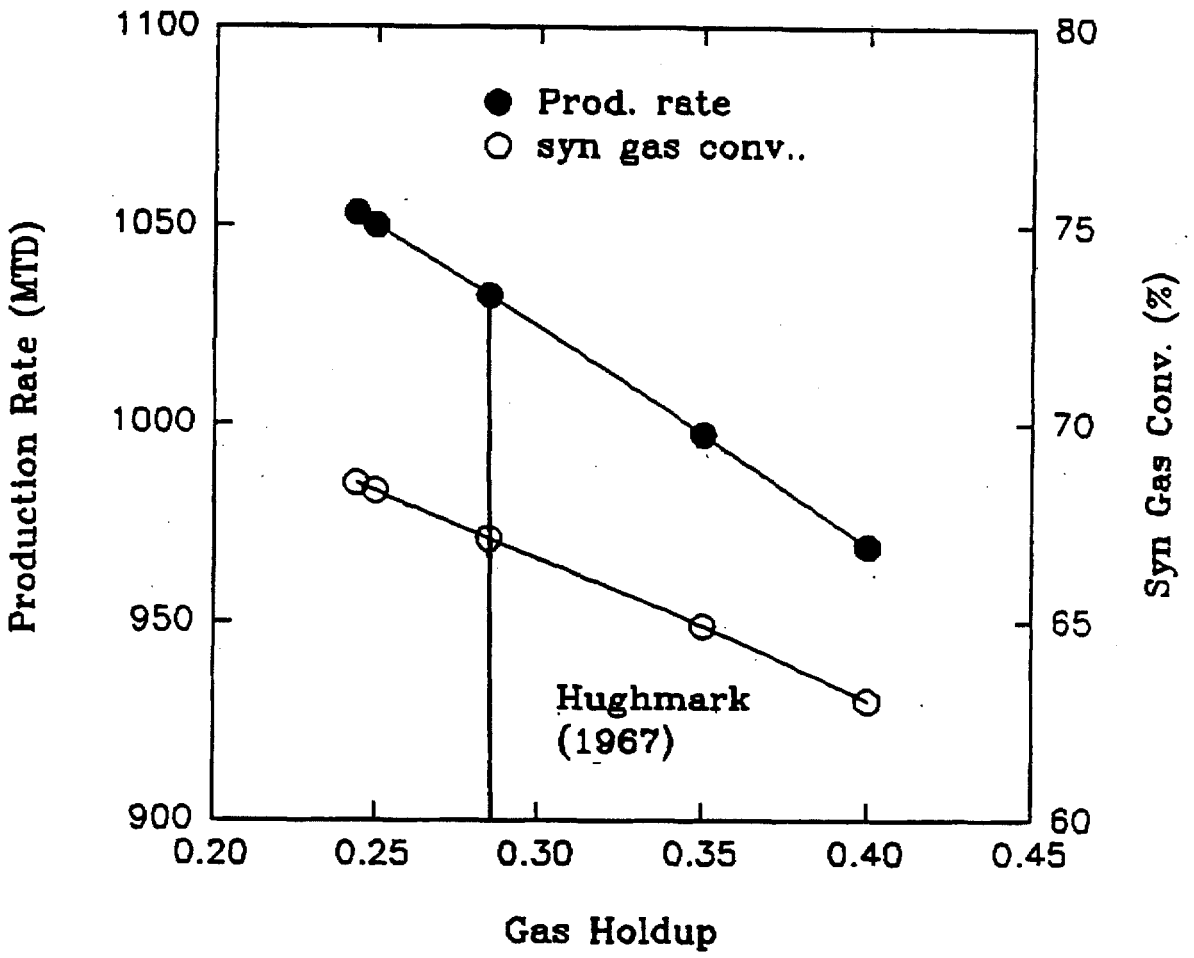

Figure 7. Effect of gas holdup on methanol production rate and hydrogen conversion

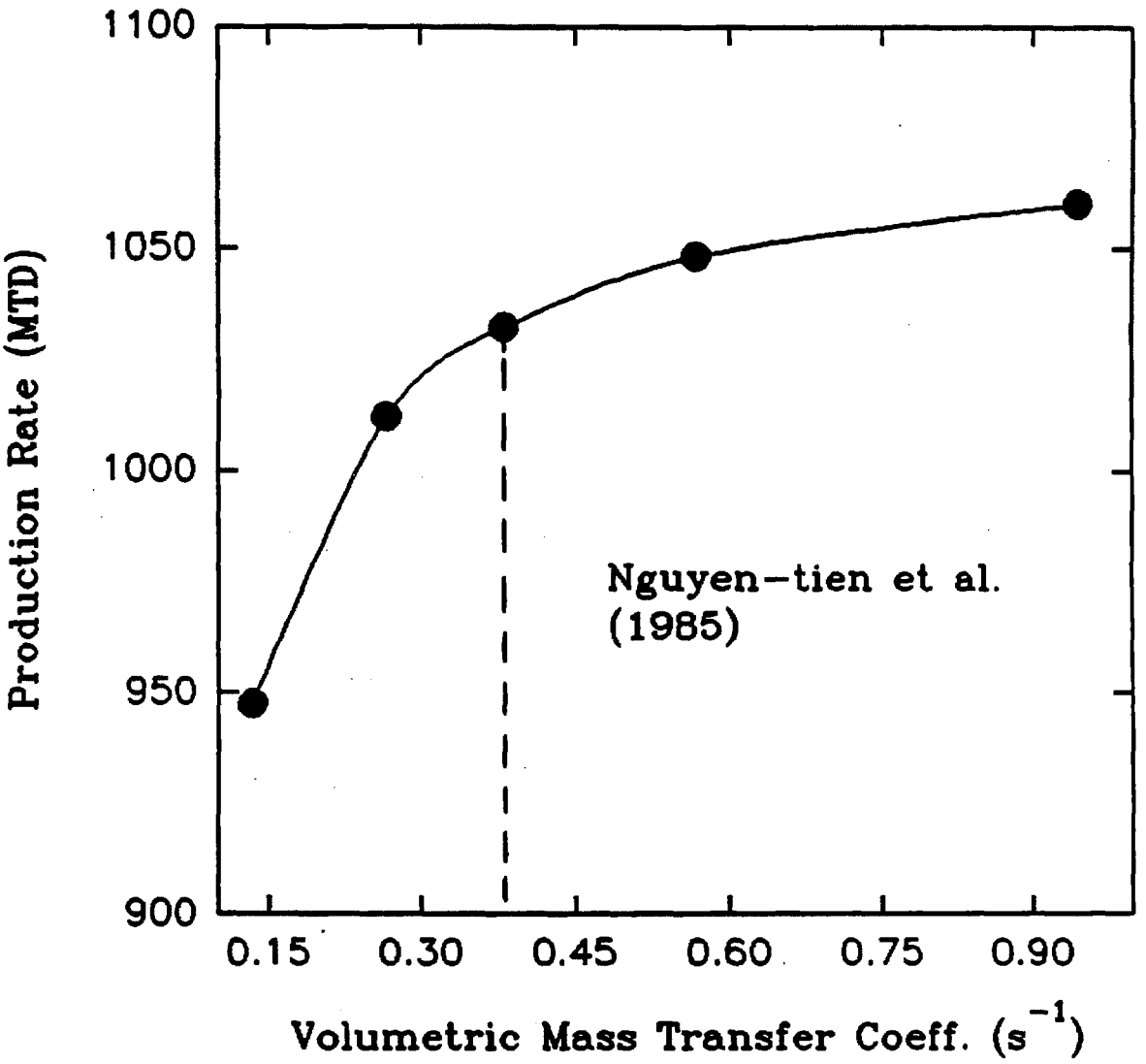

Figure 8. Effect of volumetric mass transfer coefficient on methanol production rate

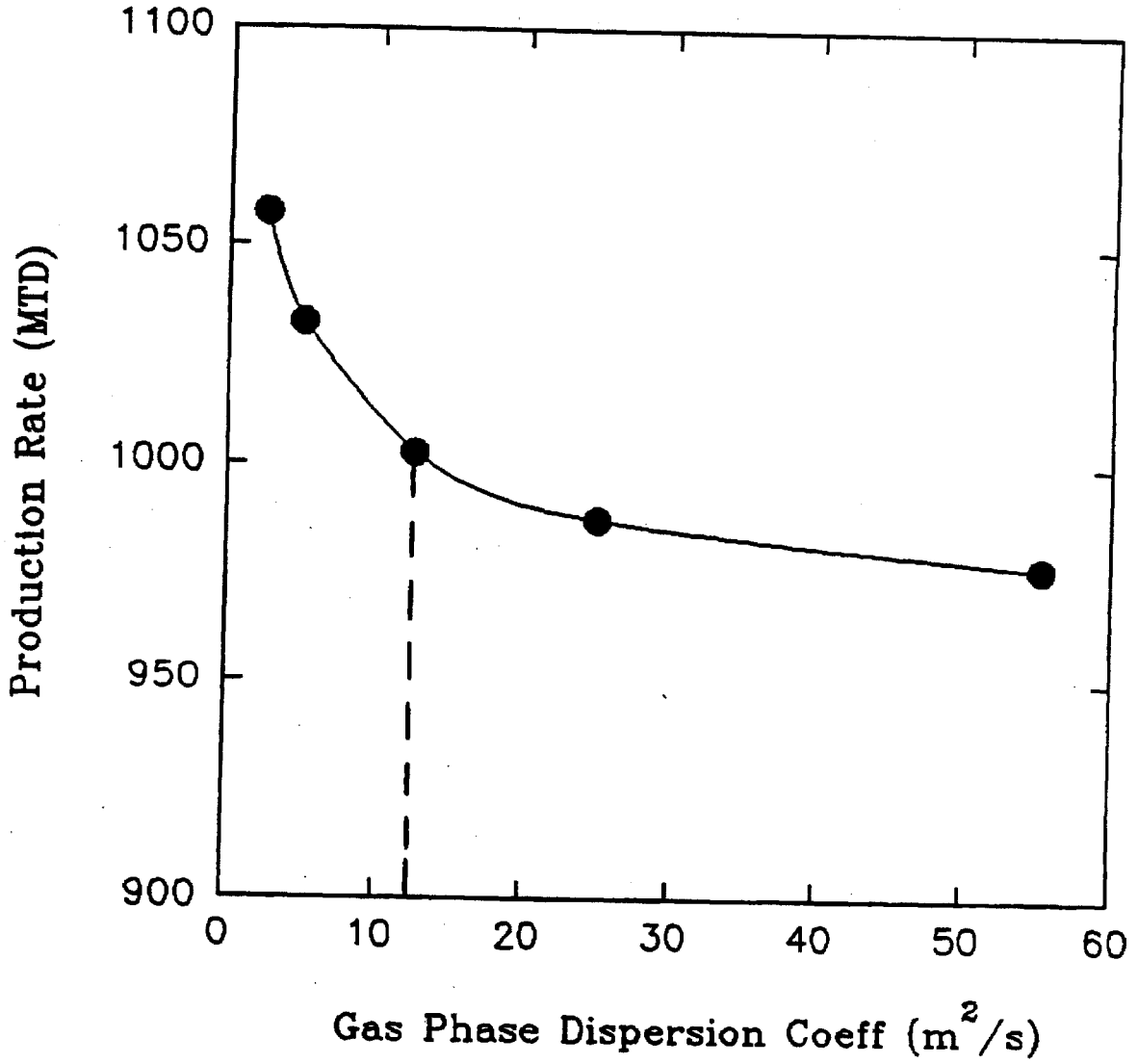

Figure 9. Effect of gas phase dispersion on methanol production rate

Fischer Tropsch Synthesis

Simulation of Demonstration Unit:

The slurry reactor model for Fischer-Tropsch synthesis was tested using the demonstration unit at Rheinpreussen. Table 5 gives the reactor dimensions and operating conditions used at Rheinpreussen and Table 6 presents simulation results. It can be seen that although, the predicted syngas conversion was 12 % higher the predicted yield of C_3^+ products was within 4%. The higher syngas conversion could be attributed to higher shift activity of the catalyst used at Rheinpreussen.

Table 5. Operating conditions and reactor dimensions for Rheinpreussen Demonstration Unit

Diameter	1.29 m
Length	7.7 m
Temperature	268°C
Pressure	11.84 atm
Gas velocity	0.095 m/s
Slurry Conc.	18 wt %

Table 6. Simulation Results for Rheinpreussen unit

	Reported	Predicted
Syngas conversion	89%	77%
STY of C_3^+ Products (kg/hr-m^3)	38.75	37.8

Simulation with Bechtel Design Data:

Bechtel presented a design for a commercial size slurry reactor for Fischer-Tropsch synthesis (Fox and Degen,1990). The slurry reactor model developed in this report was used to predict the reactor performance using Bechtel design data. Table 8 compares the reactor performance given by Bechtel study with the performance predicted by the Fischer-Tropsch reactor model developed in this report. The predicted syngas conversion is within 1% of the reported value. However, predicted production rate and space time yield are higher.

Table 7. Bechtel Design Data

Diameter	4.8 m
Length	12.0 m
Net xsect of reactor	15.16 m^2
Reactor volume	211.0 m^3
Temperature	257°C
Pressure	28.3 atm
Slurry Conc.	35 wt%
Gas velocity	0.14 m/s

Table 8. Simulation Results with Bechtel Design data

	Bechtel Design	Model Prediction
Syngas conversion	80%	79%
-CH_2- Production (MTD)	403.4	455.0
Space Time Yield (kg-CH_2-/hr-m^3)	80.	87.4

The Fischer-Tropsch reactor model was also used to investigate the effect of operating variables on reactor performance. Parameter sensitive analysis was carried out to investigate the influence of non-adjustable variables such as gas holdup, volumetric mass transfer coefficient and gas phase dispersion coefficient.

For the results of this section, the slurry reactor for Fischer-Tropsch synthesis was modeled assuming there was no external recirculation of slurry and both gas and liquid phases were axially dispersed. Table 9 gives the range of operating variables studied.

Table 9. Range of input data used to simulate slurry Fischer-Tropsch reactor

Diameter	4.5 m
Length	12.0 m
Temperature	230-270 °C
Pressure	15-20 atm
Gas Velocity	0.10-0.16 m/s
Slurry Conc.	30-35 wt.%
Syngas in Feed	90.0%
H_2/CO ratio	0.5-1.5
Particle size	0.00003-0.00005 m

Figures 10 shows that syngas conversion increased with increasing reactor temperature. Figure 11 shows that space time yield increases linearly with pressure while syngas conversion does not change significantly. Space time yield also increases almost linearly with increasing space velocity while syngas conversion decreases linearly (Figure 12). Figure 13 shows the effect of H_2/CO ratio in the feed gas on space time yield and syngas conversion. It can be seen that both pass through a maximum at a H_2/CO ratio of about 0.6 (stoichiometric).

Parameter sensitivity analysis for the reactor model was investigated for gas holdup, volumetric mass transfer coefficient and gas dispersion coefficient. Figure 14 shows that space time yield and syngas conversion decreased with increasing gas holdup. This analysis showed that a 15% error in gas holdup estimates could result in 2.0-2.5% error in the estimation of space time yields. Figure 15 shows the significance of proper estimation of volumetric mass transfer coefficient in the model. It can be seen that space time yield would be significantly reduced for low gas-liquid mass transfer rates ($k_La < 0.4\ s^{-1}$). The effect, however, becomes less significant for higher values of mass transfer coefficients. Figure 15 also shows the estimated values of volumetric mass transfer coefficients using the selected correlations. Figure 16 shows that, as expected, the space time yields and syngas conversions decrease with increasing gas phase dispersion coefficient. The gas dispersion coefficient estimated by the selected correlation in the model is also shown on the Figure. About 50% error in the estimated value of gas dispersion coefficient would result in less than 1% error in predictions for syngas conversion.

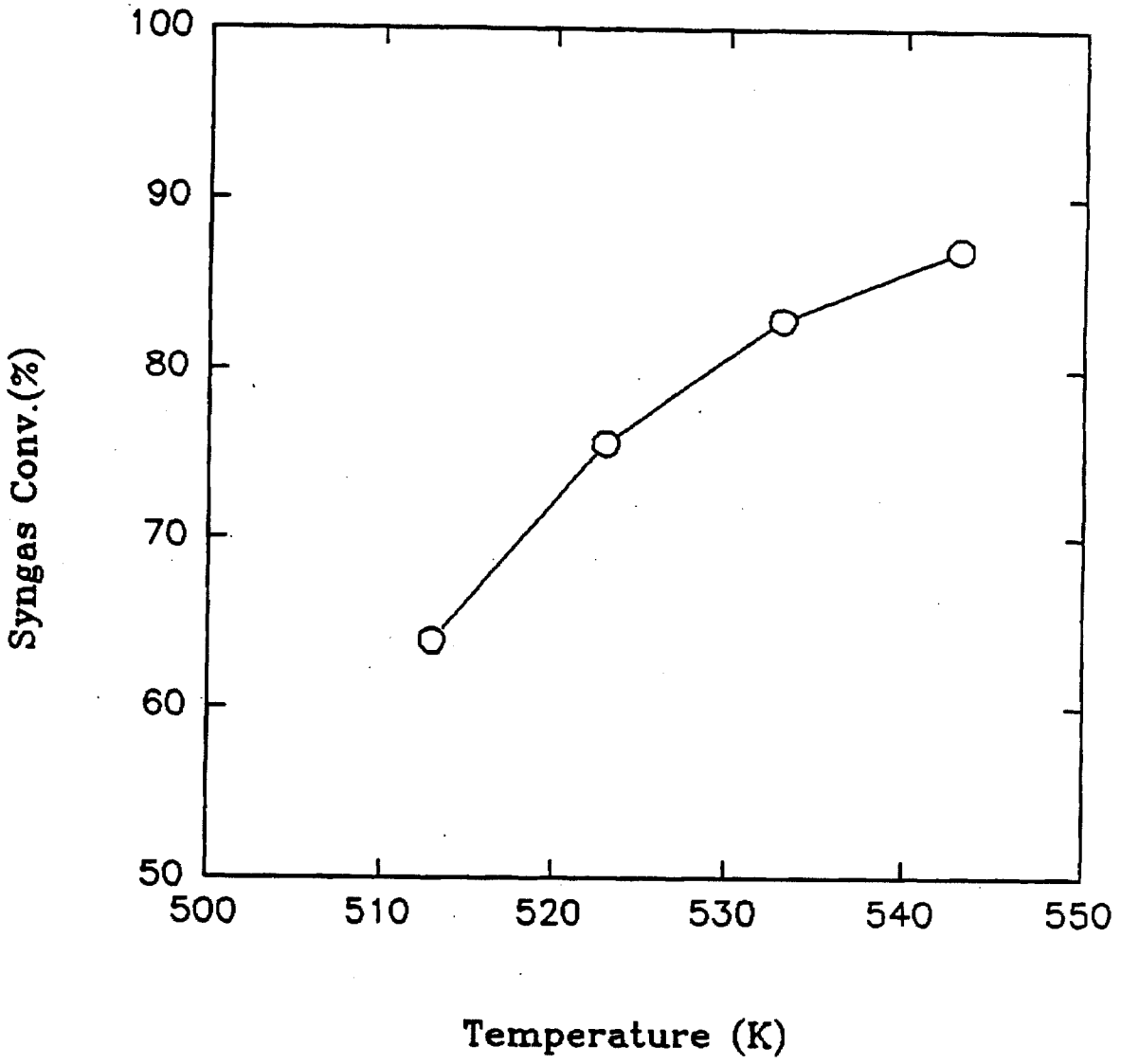

Figure 10. Effect of temperature on syngas conversion

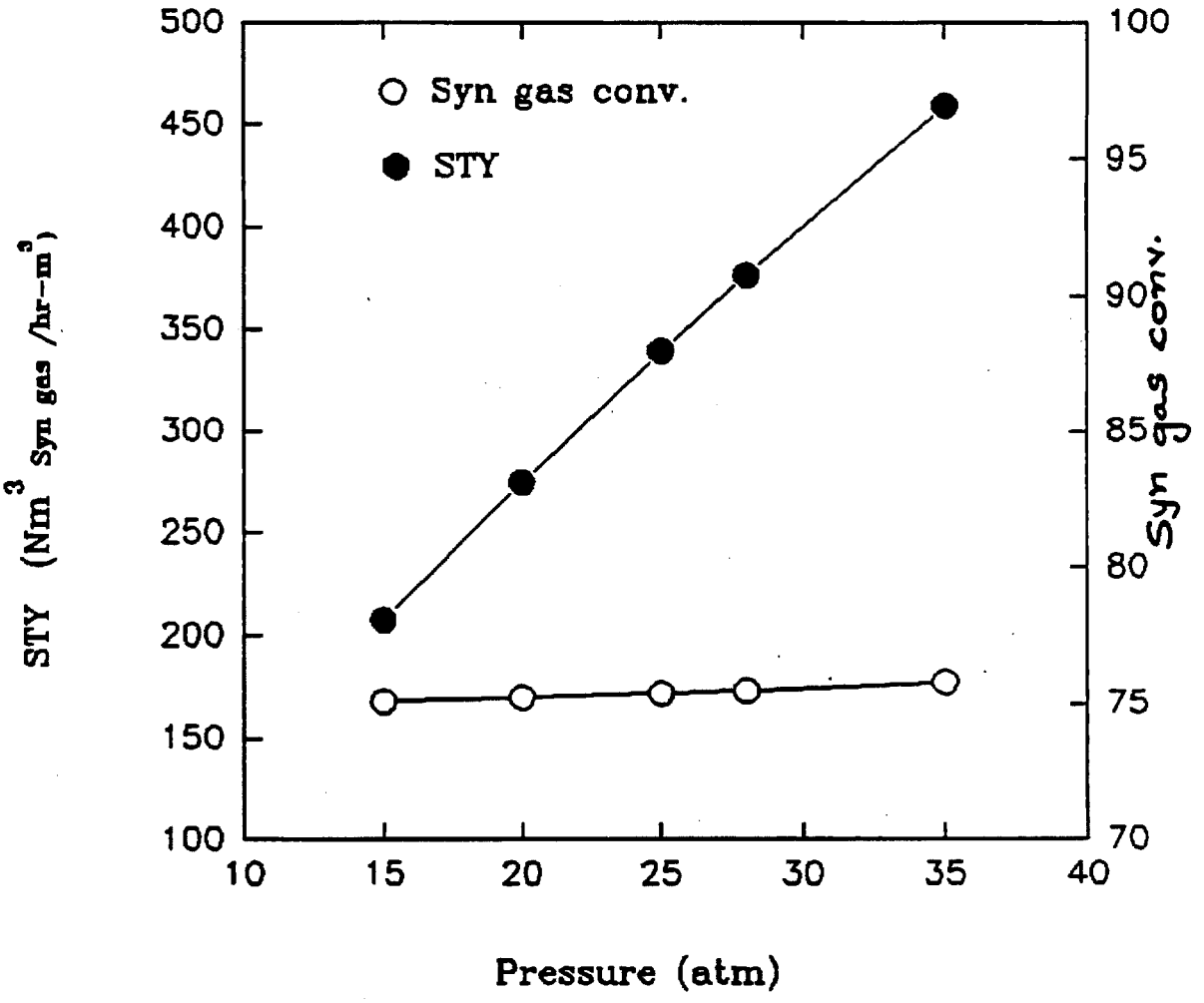

Figure 11. Effect of pressure on space time yield and syngas conversion

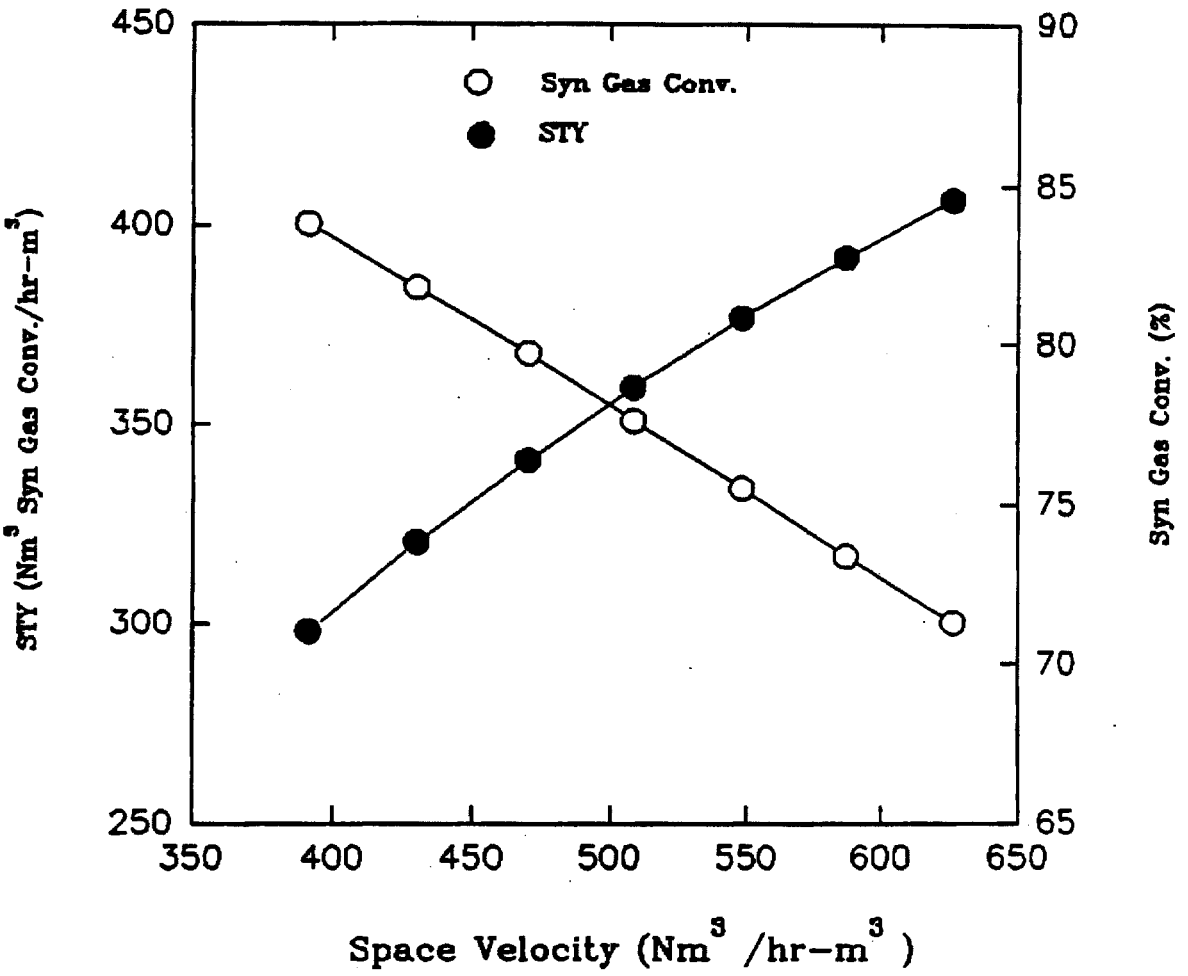

Figure 12. Effect of space velocity on space time yield and syn gas conversion

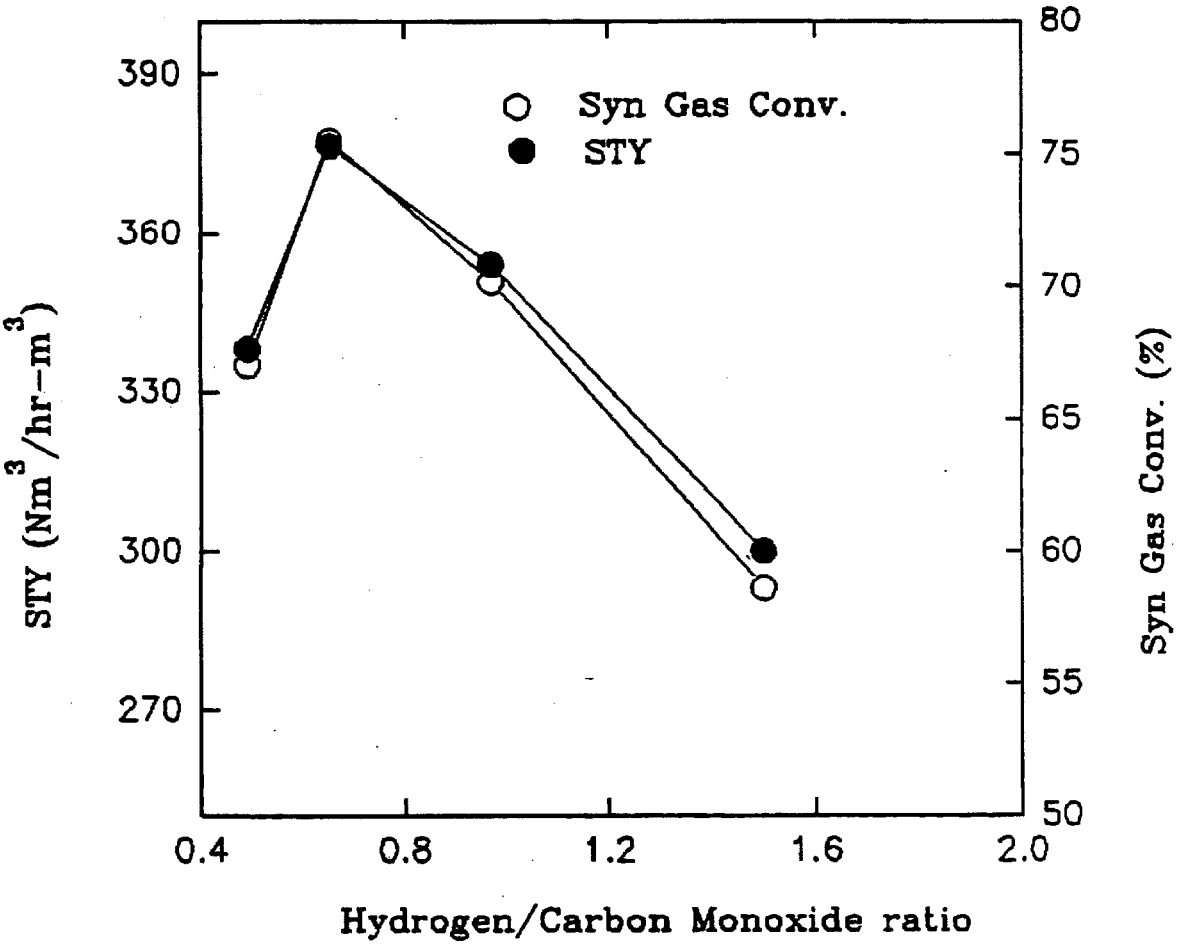

Figure 13. Effect of Hydrogen to Carbon Monoxide ratio on Syn Gas conversion

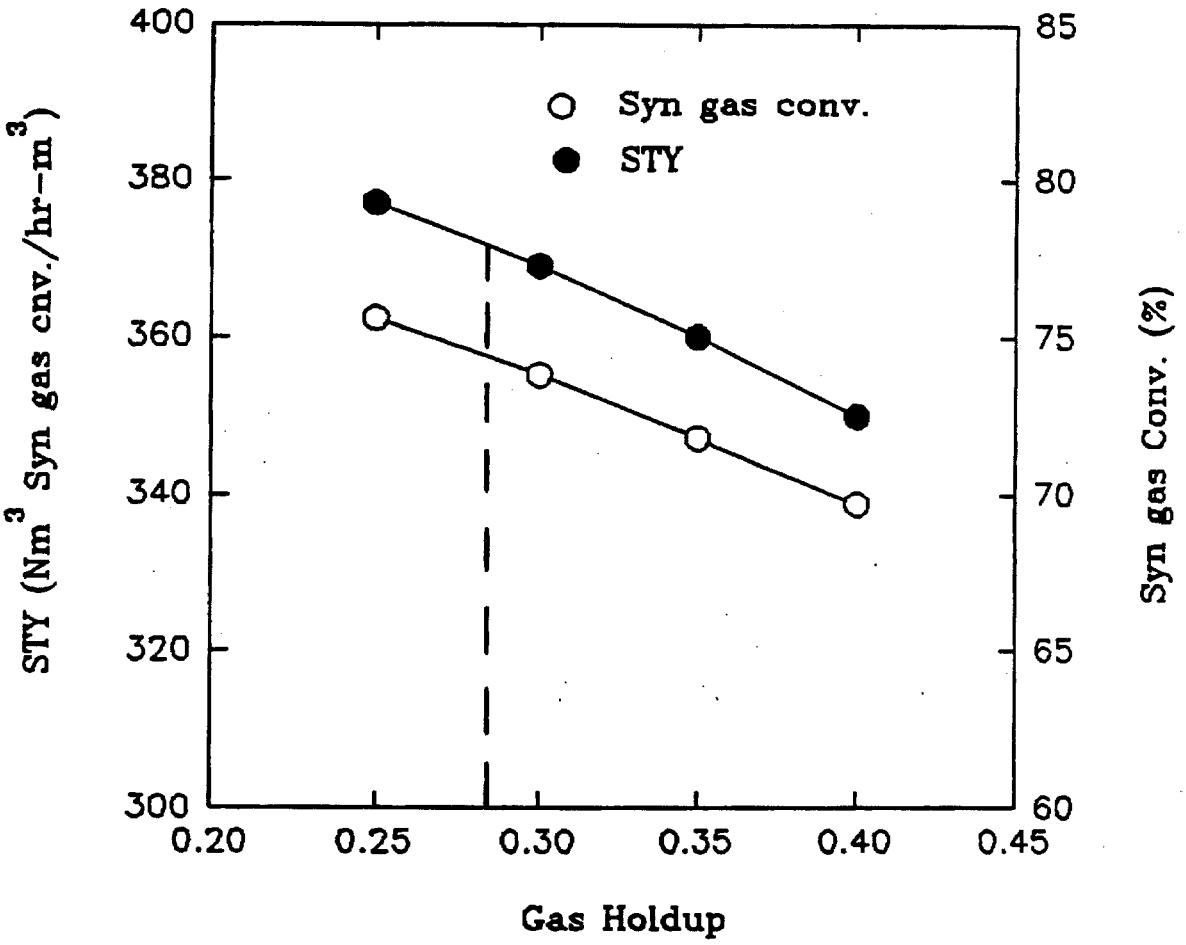

Figure 14. Effect of gas holdup on space time yield and syn gas conversion

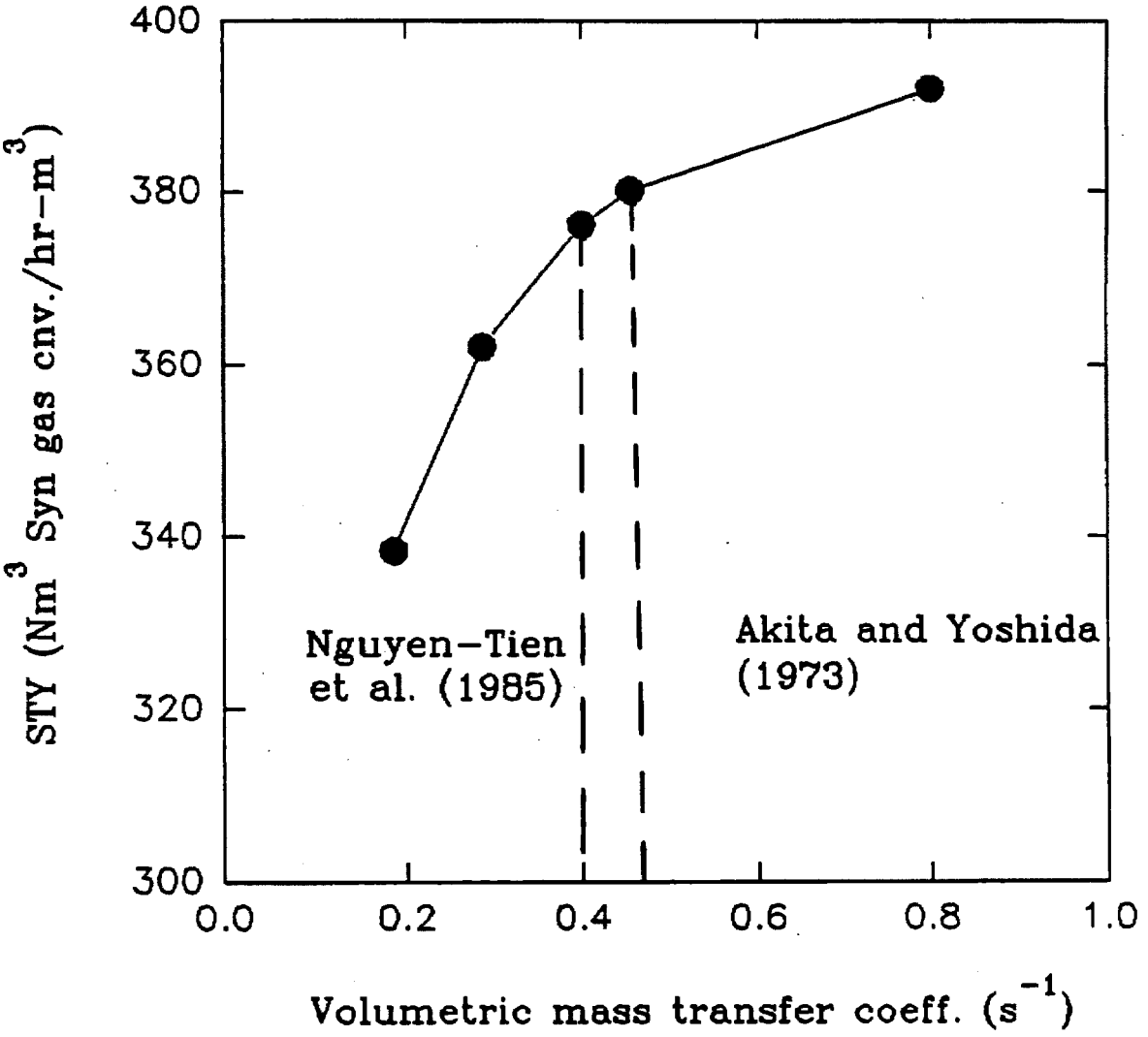

Figure 15. Effect of volumetric mass transfer coeff. on space time yield

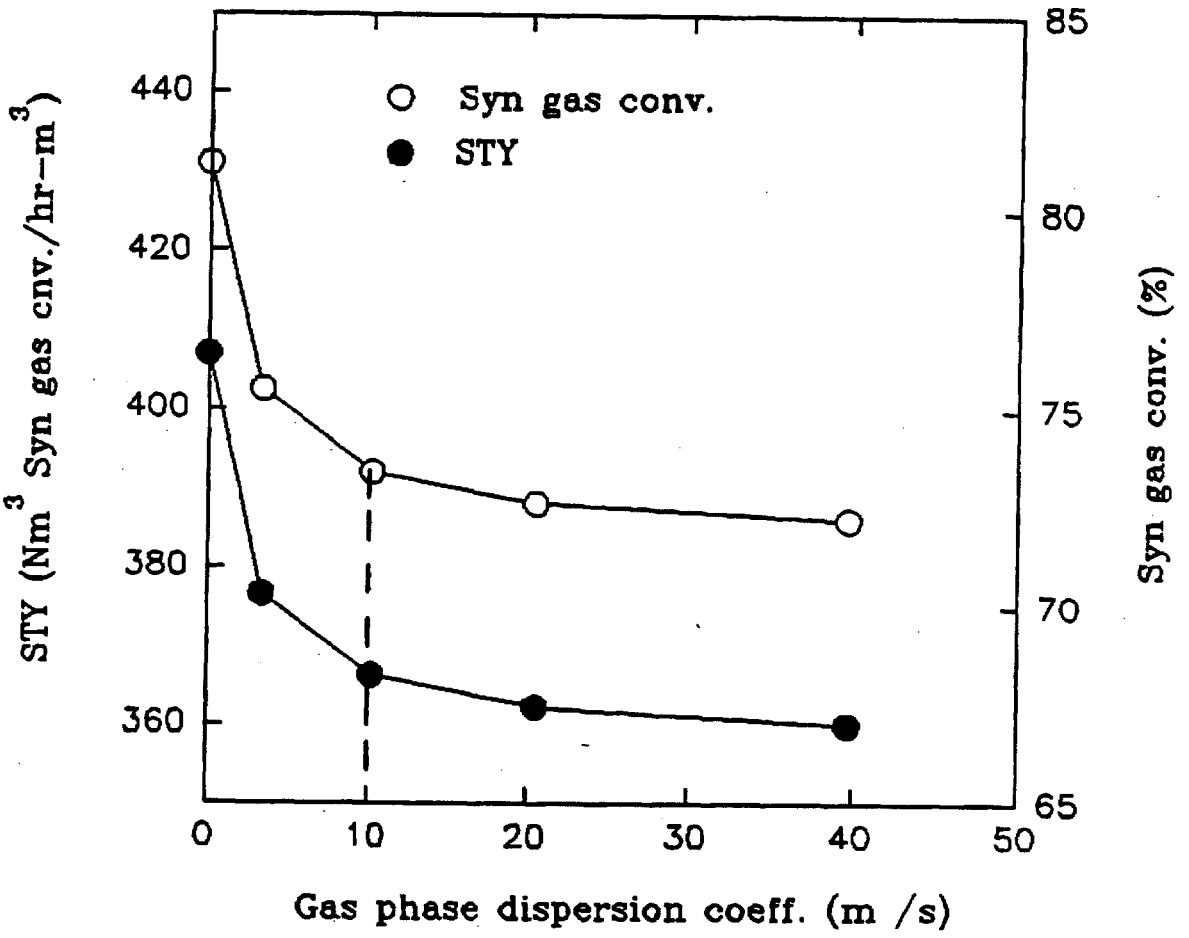

Figure 16. Effect of gas phase dispersion on space time yield and syn gas conversion